Celestial Mechanics and Dynamical Astronomy (2022) 134:33
https://doi.org/10.1007/s10569-022-10085-5

ORIGINAL ARTICLE

Comparative study of Mercuryś perihelion advance

S. P. Pogossian[1]

Received: 27 December 2021 / Revised: 4 April 2022 / Accepted: 6 May 2022
© The Author(s), under exclusive licence to Springer Nature B.V. 2022

Abstract
Mercury's motion has been studied using numerical methods in the framework of a model including only the non-relativistic Newtonian gravitational interactions of the solar system: eight major planets and Pluto in translation around the Sun. Since the true trajectory of Mercury is an open, non-planar curve, special attention to the exact definition of the advance of Mercury's perihelion has been given. For this purpose, the concepts of an extended and a geometrical perihelion have been introduced. In addition, for each orbital period, a mean ellipse was fitted to the trajectory of Mercury. I have shown that the perihelion advance of Mercury deduced from the behavior of the Laplace–Runge–Lenz vector, as well as from the extended and geometrical perihelion advance depend on the fitting time interval and for intervals of the order of 1 000 years converge to a value of $532.1''$ per century. The behavior of the perihelia, either extended or geometrical, is strongly impacted by the influence of Jupiter. The advance of the extended perihelion depends on the time step used in the calculations, while the advance of the geometrical perihelion and that deduced by the rotation of the Laplace–Runge–Lenz vector depends only slightly on it.

Keywords Gravitation · Celestial mechanics · Ephemerides · Reference systems · Planets and satellites: individual (Mercury) · (Stars): planetary systems

1 Introduction

The numerical determination of planetary orbits is one of the important tasks of modern astrophysics (Seidelmann et al. 1992, pp. 281–289). The orbit of Mercury is of particular interest since the evolution of the eccentricity of Mercury to values large enough, owing to the proximity of resonance with Jupiter, may allow collisions with telluric planets (Laskar and Gastineau 2009). Moreover, it is currently accepted that the anomalous advance of Mercury's perihelion can only be explained on the basis of general relativity (Clemence 1947; Rana

✉ S. P. Pogossian
pogossia@univ-brest.fr

[1] Université de Bretagne Occidentale, CNRS, IRD, Ifremer, IUEM, Laboratoire d'Océanographie Physique et Spatiale (LOPS), Technopôle Brest-Iroise, Rue Dumont d'Urville, Plouzané, Brest 29280, Finistère, France

Published online: 17 June 2022

1987). And yet, up to now, initiatives have been taken to shed light on some of the limitations arising from the ambiguous definition of Mercury's perihelion advance.

The central question is thus to know what kind of physical quantity is considered as being the perihelion advance and how can this be measured (Lo et al. 2013; Roy 2014; Park et al. 2017; Anderson et al. 1996). The various measurements of the perihelion advance are not perfect and have inevitable experimental errors which contribute to the uncertainty in determining this quantity (Cicalò et al. 2016; Verma et al. 2014). Optical observations of Mercury are subject to errors arising from the determination of the planet's barycenter from its visible disk (Fienga 1999). In radar measurements, uncertainties may appear due to the very weak detection signal depending on the topography of the planet, the speed, and the relative positions of the observer and the planet. As the measurement results are analyzed using one of the existing models to determine the orbital parameters, these parameters will depend on the chosen model (Verma et al. 2014; Mazarico et al. 2014). Currently, the post-Newtonian relativistic terms are automatically included in the equations of motion for the determination of the ephemeris of Mercury, which contributes to the value of the perihelion advance (Clemence 1948). In the comparisons of the Mercury perihelion advance by the different relativistic and non-relativistic models, the astronomical constants and ephemerides used in the orbital calculations based on the numerical integration of the Newtonian gravitational equations for N-bodies should be used without relativistic corrections (Le Guyader et al. 1993; Arminjon 2004). The perihelion advance of Mercury is very small, on the order of $575''$ per century ($575''/cy$), and was discovered by Le Verrier in 1859 (Le Verrier 1859).

By processing the MESSENGER ranging data, Park et al. (2017) have estimated the total precession rate of Mercury's perihelion of $575.3100''$/cy$\pm$0.0015 $''$/cy. In their estimation, (Park et al. 2017) used the parameterized post-Newtonian formalism (PPN) with fitted PPN parameters in order to extract the Mercury's precession rate from the MESSENGER ranging data. The correction provided by general relativity is smaller and is about $42.98''/cy$ (Nobili and Will 1986; Biswas and Mani 2005). The analysis of radar ranging data between 1966–1988 by Anderson et al. (1991) gives a slightly different value for the excess precession of $42.94''$/cy. Their difference $532.37''$/cy = $575.31''$/cy - $42.94''$/cy is due to influences from other planets and can be explained by Newton's classical theory of gravitation (Loskutov 2011). Different values for the perihelion advance due to the attraction of other planets of the solar system have been published by different authors and are summarized in Table 1.

Quantities that are defined in an ambiguous way can introduce uncertainties that may confuse their study. It is therefore very important to determine exactly what the perihelion advance of Mercury means for theorists, and by what methods they have calculated it in order to be able to compare their values with experimental results. Ambiguities are often

Table 1 Perihelion advance of Mercury

Reference	Perihelion advance ($''$/cy)
Misner et al. (2017)	531.54
Clemence (1947)	531.5
Rydin (2011)	531.4
Bretagnon (1982)	531.25
Narlikar and Rana (1985)	528.95
Rana (1987)	528.93
Le Verrier (1859)	526.7

found in the definitions of what is called perihelion of an orbit, using the elliptical trajectory characteristic of the two-body problem. When considering the N-body problem using the extension of the parameters characterizing the two-body motion, special attention should be paid to their physical meaning. It is for these reasons that I will reconsider in this paper a certain number of concepts which are associated with the advance of Mercury's perihelion but which have an exact definition only in the framework of the two-body problem. Their possible extensions to the N-body problem and the uncertainties and approximations that might arise from such a procedure are discussed.

I will draw special attention to the relative positions of the barycenter of the solar system, the barycenter of the two-body system of the Sun and Mercury, and the positions of the Sun and the foci of the mean elliptical trajectory of Mercury (the closest focus to the Sun). The concepts of extended and geometrical perihelia are introduced in order to give a distinct account of their advance and to compare them to the value of the perihelion advance that has been determined from the evolution of the direction of the Laplace–Runge–Lenz vector (LRL) (Stewart 2005; Goldstein et al. 2008, pp. 102–106).

2 Calculations

In present calculations, only the non-relativistic Newtonian gravitational interactions of the solar system, eight major planets, Pluto and the Sun, have been included. The ten-body Newtonian gravitational equations (including the Sun) have been integrated over a time interval of 262 144 days with a time step of about 42 minutes. It should be noted that when using this integration time interval, Mercury makes about 2 980 revolutions around the Sun, Venus 1 167 and the Earth–Moon system 718. The configuration of the solar system's four outer planets has a periodicity of about 178.7 years (62 270 days). Jose came to this conclusion (Jose 1965) by examining calculations of the solar orbit around the barycenter of the solar system. The trajectory of the Sun is considerably influenced by massive and distant planets. The period defined by Jose is slightly larger than a period of Neptune around the Sun allowing 2, 6 and 15 complete revolutions of Uranus, Saturn and Jupiter, respectively. The perihelion advance of Mercury in a time interval equal to about four Jose cycles has been analyzed, and only then the average perihelion advance per century has been calculated.

For the integration of our ten-body solar system, one needs to know the values of the basic parameters of the ten-body problem: the planet/Sun mass ratio, the Newtonian constant of universal gravitation, as well as the initial values of the positions and velocities of all the planets and the Sun. Even if the most available ephemerides are based on experimentally measured data, they include corrections based on general relativity, since the values of all the parameters depend on the model-dependent optimization procedures. Thus, Newtonian ephemeris data without relativistic corrections are required for our calculations. Le Guyader used an optimization program to subtract the relativistic corrections and the influence of the moon which correspond to the particular values of standard gravitational parameters (GM) taken from the DE200/LE200 ephemeris (Le Guyader et al. 1993). In order to obtain ephemerides without relativistic corrections, Arminjon (2004) went further by simultaneously fitting the standard gravitational parameters of planets and their initial positions and velocities. For pure Newtonian calculations, Roy (2014) used the initial positions and velocities of the planets without the relativistic corrections as calculated by Le Guyader. But for the standard gravitational parameters, Roy (2014) has used the IAU 1976 values from Taff's book (Taff 1985, p.507). In the choice of the initial values for the numerical calculations, it is necessary

to have coherence between the initial values of the orbital state vectors (three-dimensional vector for the position and for the velocity) and the standard gravitational parameters. In this study, the initial positions and velocities optimized by Le Guyader have been used, as far as the standard gravitational parameters, and the astronomical unit are concerned, their values as reported in the ephemeris DE200/LE200 (Le Guyader et al. 1993; Standish 1990) and which were used by Le Guyader during the subtraction of the relativistic corrections have been used.

A MATLAB ODE113 solver was used with RelTol=3×10^{-14} and AbsTol=10^{-16}, values that were slightly different from those recommended by Arminjon (2004) but which provide a better accuracy for the initial data first used by Le Guyader et al. (1993). The coordinates and initial velocities of the Sun, the eight major planets and Pluto at the date of the Julian ephemeris JJ = 2 451 600.5 taken from the reference (Le Guyader et al. 1993) were used. The integration results were analyzed in an invariant coordinate system related to the initial value of the barycentric linear momentum vector $\mathbf{P}_i = \sum_{i=2}^{10} M_i \mathbf{v}_i$, of eight major planets, and Pluto and the total angular momentum vector $\mathbf{L} = \sum_{i=1}^{10} \mathbf{r}_i \times \mathbf{P}_i$ of the ten-body system (Souami and Souchay 2012).

The Z-axis is directed by the direction of the total angular momentum $\mathbf{L}$. Two other vectors, $\mathbf{C}$ and $\mathbf{D}$ that are related to $\mathbf{P}$ and $\mathbf{L}$, can now be defined by the following relations: $\mathbf{C} = \mathbf{P} \times \mathbf{L}$ and $\mathbf{D} = \mathbf{C} \times \mathbf{L}$. It is assumed that the X- and Y-axes are directed, respectively, along $\mathbf{D}$ and $\mathbf{C}$. The barycenter of the solar system, composed of ten bodies, is taken as the origin of our invariant reference system. As for the barycenter of the two-body Sun–Mercury system, it practically coincides with the center of the Sun's position, and is located at a distance from the center of the Sun of only about 1.4×10^{-5} of the Sun's radius.

The maximum integration error of the MATLAB solver ODE113 has been previously analyzed (Roy 2014; Arminjon 2004) by comparing the difference between the initial values of the coordinates and velocities of the planets and their values after back and forth time integration. Figure 1a and b show the relative error of the norm of the total angular momentum and the total mechanical energy with respect to the barycenter of the ten-body solar system, respectively. These quantities are conservative. One can see that over a 700 year interval, the magnitude of the relative error of the total angular momentum and the total mechanical energy are, respectively, $\sim 10^{-14}$ and $\sim 10^{-13}$, which shows the reliability of the calculation method.

3 Results and discussion

The position and velocity vectors uniquely describe the trajectory of the body in an inertial reference frame. The Newtonian gravitational equations allow a direct numerical integration of these quantities (Arminjon 2004; Laskar 1988). In astrodynamics, it is common to use orbital elements instead of planetary positions and velocities which vary rapidly in space and time. The reason for this choice is the slow variation of the orbital elements and their simple geometrical interpretation, analogous to the Keplerian two-body problem, and assuming that the orbit for each instant is a conic section. The Keplerian orbital elements can be obtained from the position and velocity vectors by means of computer simulations (Vallado and McClain 2013, pp. 95–105). However, the evolution of the solar system is strongly influenced by the interactions between the planets and consequently these orbital elements are time-dependent, and the perturbed motion is no longer Keplerian.

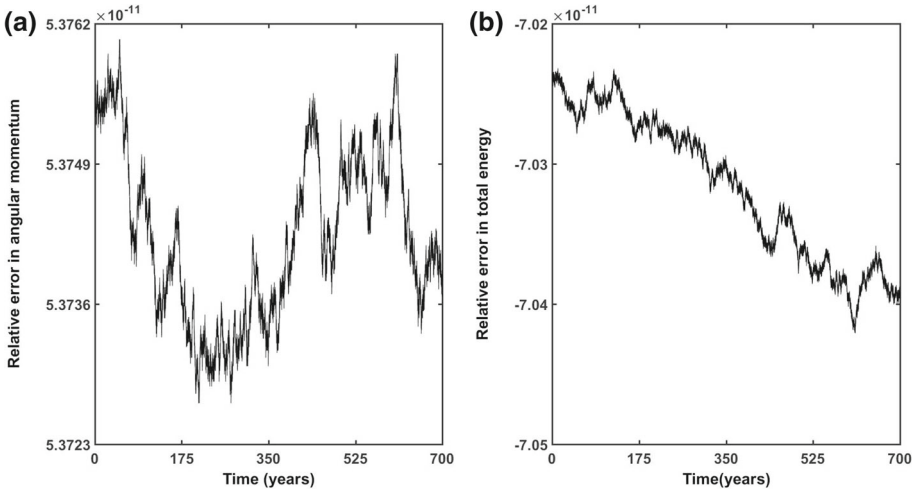

Fig. 1 In Fig. 1a, and b, the relative error of the angular momentum and the mechanical total energy in the barycentric referential of the ten-body solar system are, respectively, plotted

The inertial motion of the Sun follows a complicated trefoliar-like quasi-symmetrical Jose cycle around the barycenter of the solar system (Charvatova 1988) and changes its position relative to the foci of the mean elliptical orbit of Mercury. The question is therefore how to extend the characteristics, such as foci and apsides of a Keplerian elliptic trajectory for an N-body problem. Strictly speaking, physical quantities such as eccentricity, major axis, and the foci of Keplerian elliptical trajectories are only defined for an ellipse, and therefore, for the actual orbits of the planets of the solar system, these physical quantities are invalid.

For Keplerian orbits, the apsides remain fixed in space and the line of junction of the apsides passes through the center of attraction. For the N-body problem, this is no longer valid. The line that joins the closest point to the Sun to the farthest point from the Sun no longer passes through the center of the Sun. It rotates slowly by performing librations around the inertial reference frame associated with the barycenter of the solar system, thus breaking the axial symmetry of an elliptical orbit. Another interesting difference exists between the two-body and N-body Keplerian orbits concerning the closest and farthest points from the Sun. For Keplerian orbits, the distance to the center of attraction is minimal and the velocity is maximal at the perihelion; conversely, the distance to the center of attraction is maximal and the velocity is minimal at the aphelion. For non-Keplerian orbits with N bodies, at the closest (or farthest) distance from the attracting body, the velocity of a planet is not maximal (or minimal). This is why several characteristics of an open evolutionary orbit should be reconsidered, since their exact definition is only valid for a two-body Keplerian problem.

Different orbital characteristics of the two-body Keplerian problem will be now extended to the orbits of the ten-body solar system. For example, the sidereal orbital period of a planet can be defined as the time between two transits of the planet at the same point relative to the fixed stars. This definition must be slightly modified if the planet has an evolving orbit under the influence of other planets. The trajectory is open and therefore the planet passes through different points at each revolution. One can then introduce the concept of the mean Fourier period $T_{Fourier}$ as the dominant peak of the spectral power (Fourier transform) of the angle of the barycentric position vector of Mercury and the X (or Y) axis of the barycentric reference system in a time interval allowing a very large number of revolutions of Mercury

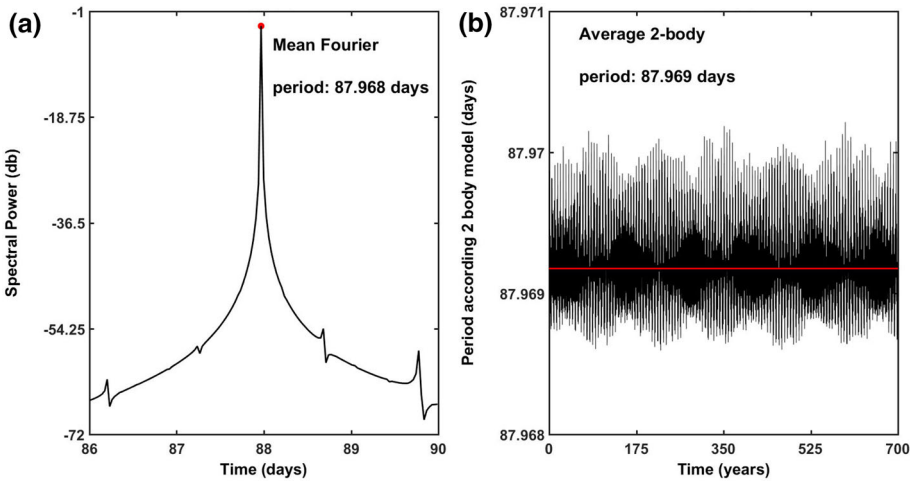

Fig. 2 Figure 2a shows the spectral power (in db) of the Fourier transform of the Mercury–Sun distance in a time interval of 262 144 days which permits a very large number of revolutions (2980) of Mercury around the Sun. The red circle shows the position of the dominant peak. As shown in Fig. 2a, the period defined by the dominant peak of the Fourier transform is equal to $T_{Fourier} = 87.968$ days. The periods calculated from Eq. (3) based on the two-body model are shown in Fig. 2b. The average period obtained with this method gives: $T_{2-body} = 87.969$

around the Sun. Note that during the time interval of 262 144 days Mercury makes about 2 980 revolutions around the Sun. Figure 2a shows that the mean Fourier period as defined above is equal to $T_{Fourier}$=87.968 days. The chosen time interval 262 144=2^{18} is convenient for the fast Fourier transform (fft). Note that this time interval is slightly longer than four Jose cycles: 262 144 days$\approx$ 717.7 years$\approx 4\times 179$ years.

This value can be compared with the mean orbital two-body period defined by analogy with the two-body problem T^m_{2-body}=87.969 days as shown in Fig. 2b. These two mean periods are slightly different, $T^m_{2-body} \neq T_{Fourrier}$ and for a more exhaustive analysis the larger of these two mean periods will be used, which allows us to always include a closest and a farthest point of approach to the Sun in the interval of a mean period. It should be noted that depending on the number of iterations per year and the number of revolutions of Mercury taken into account, the maximum value is sometimes the mean Fourier period and sometimes the average two-body period. Once the mean orbital period has been chosen by the method described above, one can fix on for the initial reference time, an arbitrary instant which is different from the time of perihelion passage.

By definition, the perihelion of a planet in the two-body problem is the closest point of approach to the Sun of its elliptical trajectory (Sun is considered to be at one of foci of elliptical trajectory). In such a definition of perihelion, all the points of the elliptical trajectory implicitly play a role since the perihelion must be the closest point to the Sun among all the other points. The concept of perihelion can be extended to open trajectories close to the ellipse and known at least on one mean period (as defined above). Thus, the extended perihelion is the closest point to the Sun among all the other points of a quasi-elliptical trajectory of the same mean period. In the same way, the extended aphelion is defined as the farthest point from the Sun among all the other points of a quasi-elliptic trajectory of the same mean period. The direction of the extended major axis for each mean period will then be considered as the direction of the vector connecting the Sun to the extended perihelion. It should be noted that

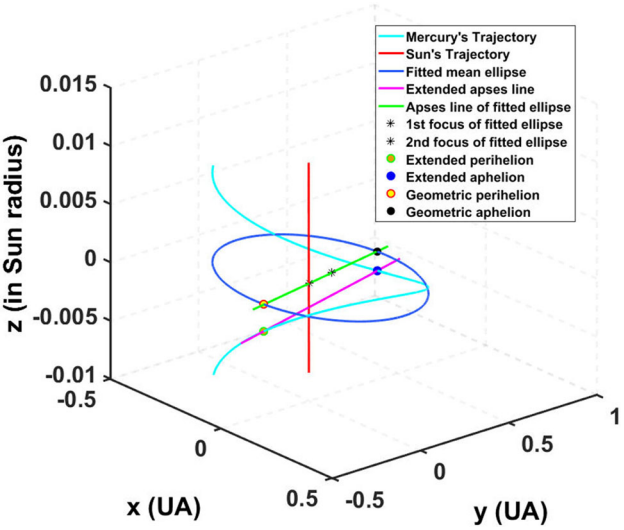

Fig. 3 In Fig. 3, the open trajectory of Mercury (curve in cyan) in the time interval of one mean period is plotted. The line of the apsides of the fitted mean ellipse is represented by the green color segment. The extended line of the apsides joining the extended perihelion (orange color filled circle with green edge color) to the extended aphelion (blue color filled circle) is represented by the magenta color segment

lines joining, respectively, the extended perihelion and the extended aphelion to the Sun are not collinear. The average angle between these two directions is about 179.955°. Moreover, the straight line joining the extended perihelion and the extended aphelion (extended line of apsides, or extended apsides line) no longer passes through the center of the Sun. The extended perihelion and the extended aphelion have no fixed position and undergo slow and variable oscillations of very long periods.

As shown in Fig. 3 (cyan curve), the trajectory of Mercury even if it is close to an ellipse, it remains an open curve. The Z-axis of Fig. 3 is drawn to the scale of the radius of the Sun: $D = 4.65\,047 \times 10^{-3}$ AU in order to visualize the opening of the ellipse of about 10^{-4} AU. The trajectory of the Sun follows the red line in Fig. 3. It is important to define the mean elliptical trajectory associated with the quasi-elliptical orbit of Mercury as a mean ellipse over the mean period in analogy with the two-body problem (blue curve). Since all the points of the trajectory are not co-planar, a plane is first fitted to the points of the trajectory over one mean period starting from the initial reference time, as shown in Fig. 4. (The plane is shown in light brown color.) All the points of the trajectory are projected into this plane, and then an ellipse (in blue color in Figs. 3 and 4) is fitted to all the projected points of the mean period in the sense of a least squares fit. The foci of such a mean ellipse are then determined (star points in black color in Fig. 4). In Fig. 3, the line of apsides of this mean ellipse is represented by the green segment. The major axis of the mean ellipse is co-linear with the apsides line of the latter.

The extended line of the apsides joining the extended perihelion (a orange color filled circle with green edge color on the trajectory of Mercury Fig. 3) to the extended aphelion (blue color filled circle on the trajectory of Mercury) is represented by the magenta colored segment. It can be seen that the major axis of the mean ellipse and the extended line of the apsides are not parallel and are spatially separated in the scale shown on the Z-axis in Fig. 3. Therefore, in addition to the extended perihelion, the geometrical perihelion will be defined

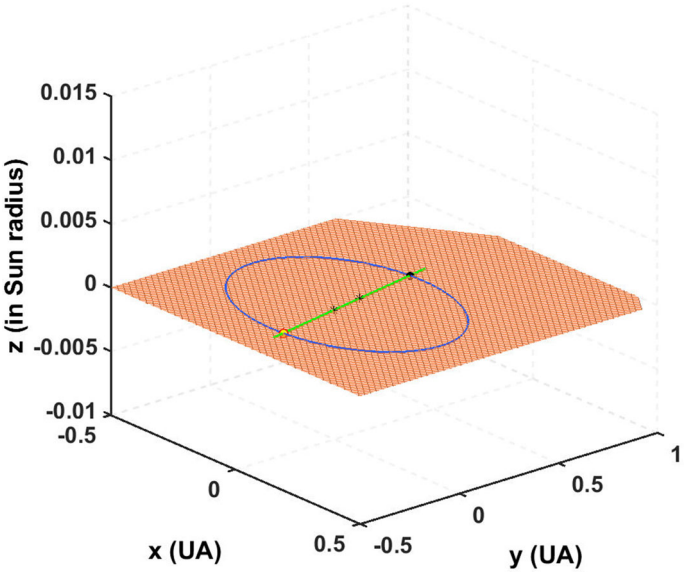

Fig. 4 In Fig. 4, the mean orbital plane fitted to the points of the trajectory (which are not coplanar) in the time interval of one mean period is plotted in light brown color. An ellipse (shown in blue in Fig. 4) is fitted to all the trajectory points projected onto this mean plane in the sense of a least squares fit. The perihelion (yellow color filled circle with red edge color) and aphelion (black color filled circle) of this ellipse as well as its two foci (star points in black color) are also represented

as the point of the mean ellipse closest to the focus of the mean ellipse which is closest to the Sun. The geometrical perihelion is plotted in Fig. 4, as a yellow color filled circle with red edge color, while the extended perihelion is represented in Fig. 3 with orange color filled circle with green edge color. For the two-body problem, the directions of the extended perihelion and the geometrical perihelion coincide. But for the N-body problem with $N \geq 3$, these directions are distinct, and their motion with respect to an inertial coordinate system must be evaluated separately.

It is important to underline that the concept of an average trajectory appears as soon as one deals with small deviations from a well identified behavior. For example, in the description of the slow evolution of the orbital elements by the Lagrangian planetary equations, one uses the Lagrangian constraints. But instead of Lagrangian constraints, one can also use other constraints by reformulating new planetary equations called generalized gauge equations (Efroimsky and Goldreich 2004). Gurfil (2004) extended the generalized constraints by presenting an averaged form of the gauge-generalized planetary equations with average classical orbital elements.

The advance of the extended perihelion and the geometrical perihelion can be characterized by the angle of rotation of the radius vectors pointing, respectively, to these perihelia with respect to a predefined reference direction. The advances of these extended and geometric perihelia can be thus compared to the angle of rotation of the direction of the LRL vector with respect to this same reference vector.

In a large number of works the advance of Mercury's perihelion is predominantly represented with the rotation of the LRL vector (Davies 1983; Goldstein et al. 2008, pp. 102–106). In the two-body problem, this vector lies in the plane of the elliptical orbit, and is parallel to

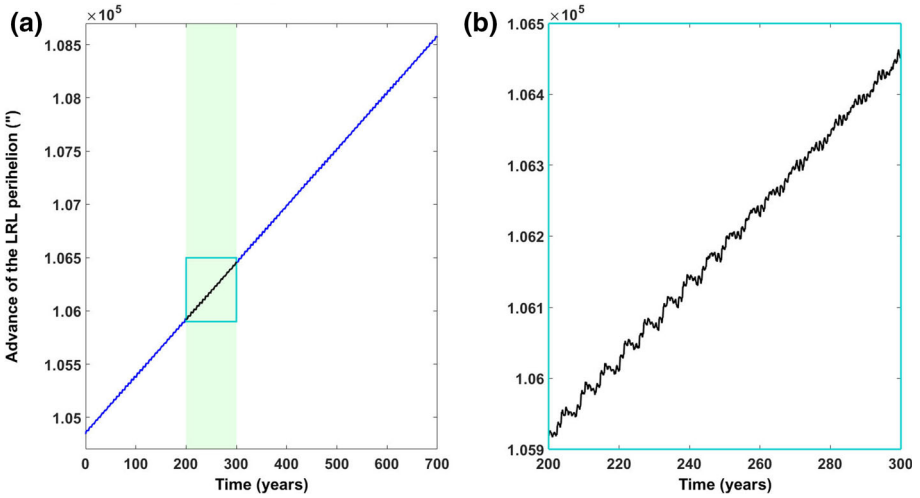

Fig. 5 In Fig. 5a, the angle (in angular seconds) between the reference vector and the direction of the LRL vector is plotted as a function of time. In Fig. 5b, a close-up picture of this evolution in a time interval of one century is presented

the major axis and points in the direction of the perihelion (Stewart 2005). Frequently, the rotation of the LRL vector is also used to estimate the contribution of general relativity to the perihelion precession of a planetary orbit (Landau and Lifšic 2010, p. 370; Weinberg 1972, pp. 230–233; Garavaglia 1987). However, in the case of the N-body problem, the secular rotation of this vector cannot be clearly identified with the advance of Mercury's perihelion (Ebner 1985).

The LRL vector can be evaluated at each point of the trajectory as soon as the evolution of the position and velocity vectors in time is known. The LRL vector is noted by **A** in this work. In the case of the two-body problem, **A** is a constant vector parallel to the major axis and is directed toward the perihelion:

$$\mathbf{A} = \left(\frac{M_\odot M_M}{M_\odot + M_M}\right)^2 \left[\left(v_M^2 - \frac{GM_\odot + GM_M}{r_M}\right)\mathbf{r}_M - (\mathbf{r}_M \cdot \mathbf{v}_M)\,\mathbf{v}_M\right], \tag{1}$$

where $\mathbf{r}_M$ and $\mathbf{v}_M$ are, respectively, heliocentric position and velocity vectors of Mercury.

For the N-body problem, the LRL vector becomes a continuous function of time. In order to represent the rotation of this vector, it is necessary to follow its evolution with respect to a fixed reference direction. We can define the fixed direction of reference as the line of intersection of two instantaneous orbital planes: the initial osculating orbit plane of Mercury and the initial ecliptic plane. The mean advance of the perihelion is generally estimated over a period of a century, during which Mercury makes 415 revolutions around the Sun. The linear least squares regression of the perihelion advance over a selected fitting time interval that may be longer than one century produces a trend line. Then, the advance of the perihelion over a century is calculated by the help of linear fit coefficients. The angle of rotation between the direction of the LRL vector and the reference direction is shown in Fig. 5a. Figure 5b shows a close-up picture of this evolution over a time interval of one century. This characteristic behavior is identical to the curves presented by Narlikar and Rana (1985).

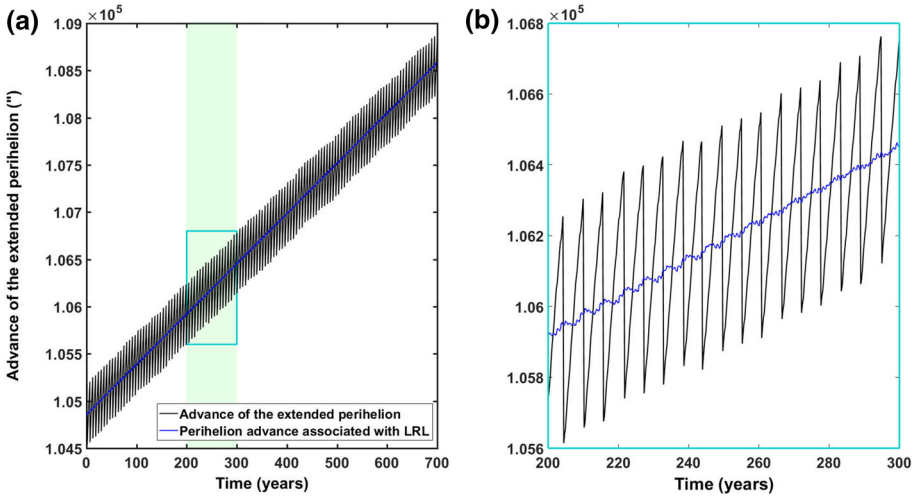

Fig. 6 In Fig. 6a and b, the extended perihelion advance is plotted as a function of time. A close-up of the behavior of this evolution in a time interval of one century is illustrated in Fig. 6b. The time evolution of the LRL vector defined perihelion advance is also added in blue color in Fig. 6a and b for comparison purposes

The advance of the perihelion as defined by the LRL vector will be compared with the advances of the extended and geometrical perihelia. For the two-body problem, the direction of the LRL vector defined by Eq. (1), and the direction of the extended perihelia coincide.

The advance of the extended perihelion can be calculated as the angle between the fixed reference direction and the position vector pointing to the extended perihelion at successive mean periods. In Fig. 6a and b, an oscillatory behavior of the extended perihelion advance with an amplitude of about $700''$ can be observed. Nevertheless, one can always note a linear increase trend of the average advance of the extended perihelion. LRL vector is added in blue in Fig. 6a and b for comparison purposes.

As defined above, the geometrical perihelion is the point of the mean ellipse closest to one of the foci (closest to the Sun) of the mean ellipse. For the two-body problem, the direction of the LRL vector and the direction of the geometrical perihelion coincide. The geometrical perihelion advance is calculated as the angle between the reference direction and the vector pointing from the focus closest to the Sun of the mean ellipse to the point of the ellipse closest to this focus for each successive mean period. In Fig. 7a and b, the evolution of the advance of the geometrical perihelion is presented.

The mean amplitude of the oscillatory behavior of the geometrical perihelion advance is about $3700''$. Despite the greater amplitude of the oscillations of geometrical perihelion advance, a linear trend of the increase if the mean geometrical perihelion advance is still observed. The time-dependent LRL vector is also plotted in blue in Fig. 7a and b for comparison purposes. It should be noted that the amplitude of the oscillatory behavior of extended and geometrical perihelia are different by a factor of about 5.

In Fig. 8a, b and c, a Fourier analysis has been performed, evaluating the spectral power of the perihelion advance associated with the rotation of the LRL vector with respect to the fixed reference direction as well as to extended and geometrical perihelion advances. As shown in Fig. 8a, the spectral power of the perihelion advance as defined by the LRL vector is almost independent from the motion of Jupiter, while the extended and geometrical perihelion advances depend strongly on it (Fig. 8b and c). There is a striking difference

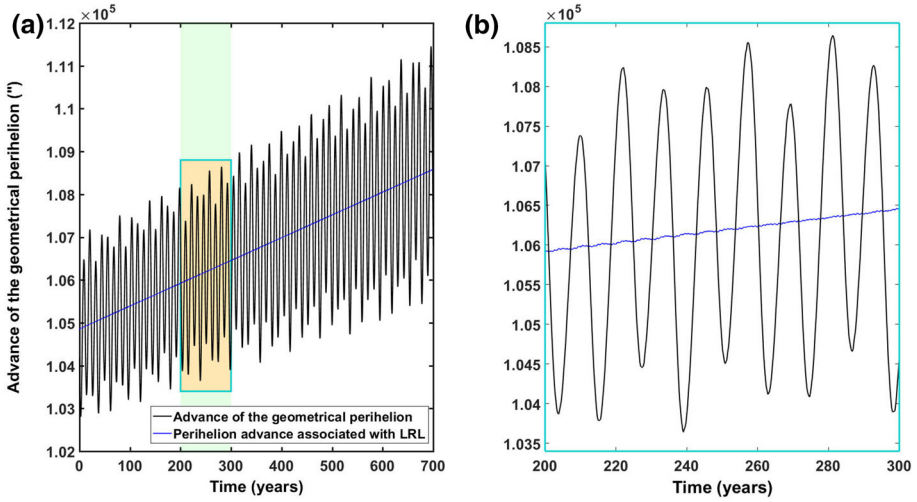

Fig. 7 Figure 7a and b demonstrate the behavior of the geometric perihelion advance as a function of time. A closer look at the behavior of this evolution in a time interval of one century is illustrated in Fig. 7b. The time evolution of the LRL-vector-defined perihelion advance is also added in blue color in Fig. 7a and b for comparison purposes

between the spectral powers of the advances of the extended and geometric perihelia, since the spectral power of the extended perihelion depends strongly on the half-period of Jupiter's revolution around the Sun (Fig. 8b), whereas that of the geometrical perihelion depends on Jupiter's period (Fig. 8c). In order to clarify the determination of average perihelion advance per century of Mercury, I compared the influence of the fitting time interval on the mean perihelion advances associated with the rotation of the LRL vector, the extended and geometrical perihelia.

The mean amplitude of the oscillatory behavior of the geometrical perihelion advance of Mercury is very large about $3700''$. The mean amplitude of the oscillations of the extended perihelion is about $700''$ (about 5 times smaller), while the mean amplitude of the oscillations of the advance of the perihelion associated with the LRL vector is only about $30''$.

In order to describe the dependence of the mean perihelion advance per century on the fitting time interval, the evolution of the mean advance per century of the extended, geometrical and LRL vector defined perihelia for three different calculation intervals: 520 years, 718 years and 1011 years are, respectively, plotted in Figs. 9, 10 and 11.

All the curves in Figs. 9, 10 and 11 show a convergence tendency of the all mean perihelia advances per century toward a value of $532.1''$/cy. It should be noted, however, that the mean perihelion advance per century as defined by the rotation of the LRL vector converges very rapidly to an average value of $532.1''$/cy, while the convergence of the mean extended perihelion advance per century is slower. Naturally, the slowest convergence is that of the mean geometrical perihelion advance per century because of the oscillatory character of greater amplitude. It should be noted that the shape of different mean perihelion advances per century for short fitting periods may depend on the number of points used in the integration. This dependence on the number of points used in the integration over an integration period of 1011 years is illustrated in Fig. 12a, b and c.

The mean perihelion advance per century as defined by the rotation of the LRL vector shows a very weak dependence on the time iteration step. The mean geometrical perihelion

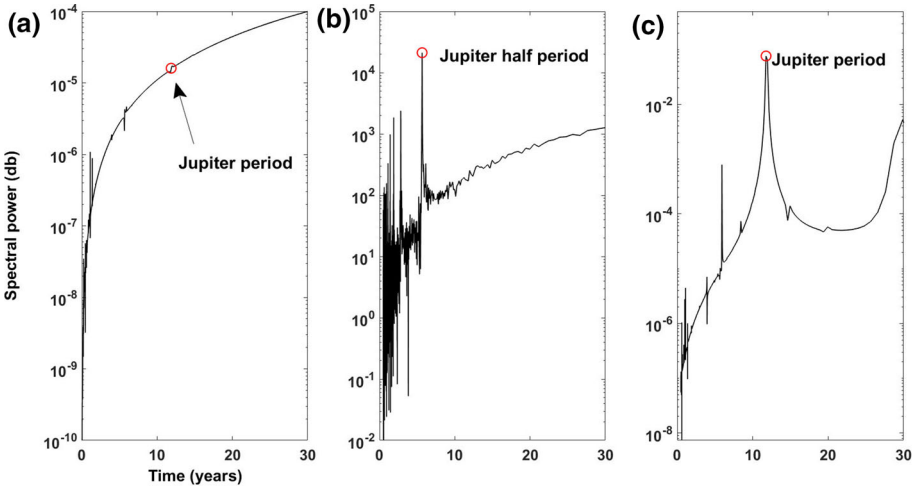

Fig. 8 In Fig. 8a, b and c, a Fourier analysis of LRL, extended and geometrical perihelia are, respectively, performed. The spectral power (in db) of the advance of extended and geometrical perihelia (Fig. 8b and c) as well as the perihelion advance associated with the rotation of the LRL vector (Fig. 8a) with respect to the fixed reference direction as a function of the inverse of the frequency is plotted

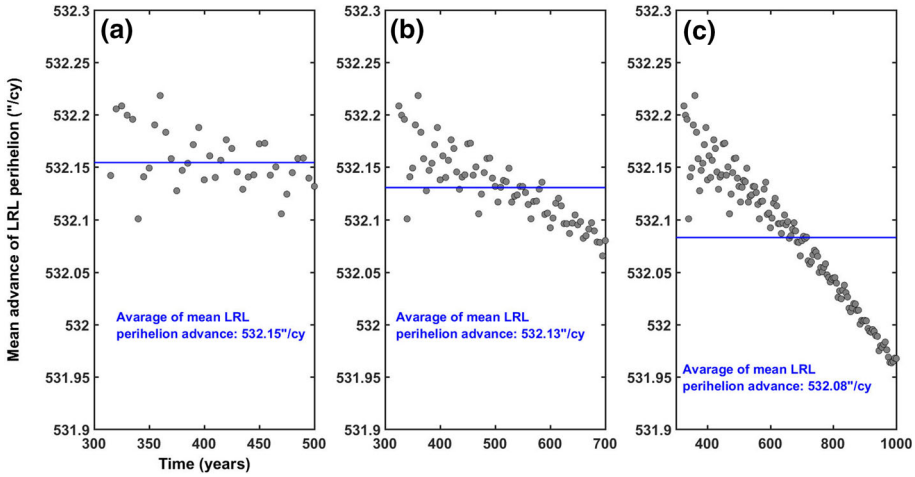

Fig. 9 Perihelion advance deduced by the rotation of the LRL vector is fitted by the least squares method to a linear function. In Fig. 9a, b and c, the mean perihelion advance over a century is deduced by the fitting coefficients as a function of the fitting time interval for three different calculation intervals: 520 years, 718 years and 1011 years, respectively. For each interval, the calculation of the mean advance of the perihelion per century is started on an initial fitting time period of 300 years, which is gradually increased with a step of 5 years

advance per century also shows a very weak sensitivity to the time step. The mean extended perihelion advance per century is much more sensitive to the time step, and for higher fitting time intervals, there will be a convergence to the same value of $532.1''$/cy which was predicted by the rotation of the LRL vector.

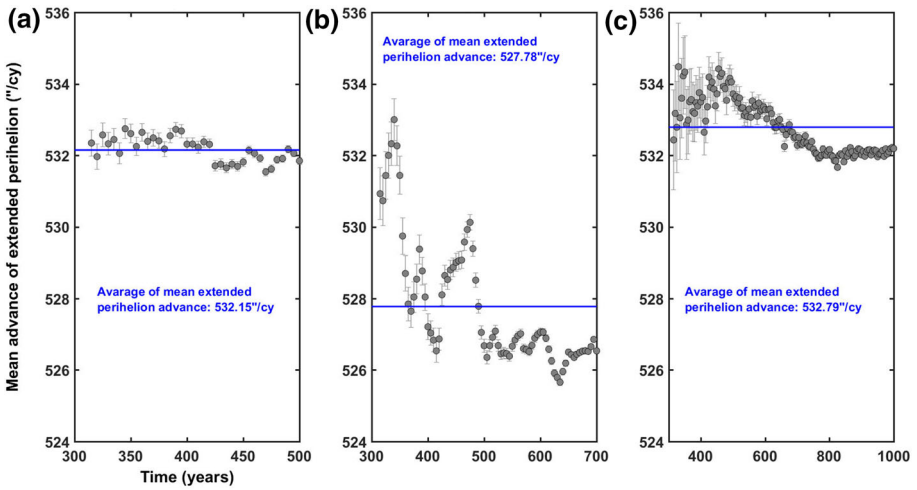

Fig. 10 Advance of the extended perihelion is fitted by the least squares method to a linear function. In Fig. 10a, b and c, the mean perihelion advance over a century is deduced by the help of fitting coefficients as a function of the fitting time interval for three different calculation intervals: 520 years, 718 years and 1011 years, respectively. For each interval, the calculation of the mean advance of the perihelion per century is started on an initial fitting time period of 300 years, which is gradually increased with steps of 5 year intervals

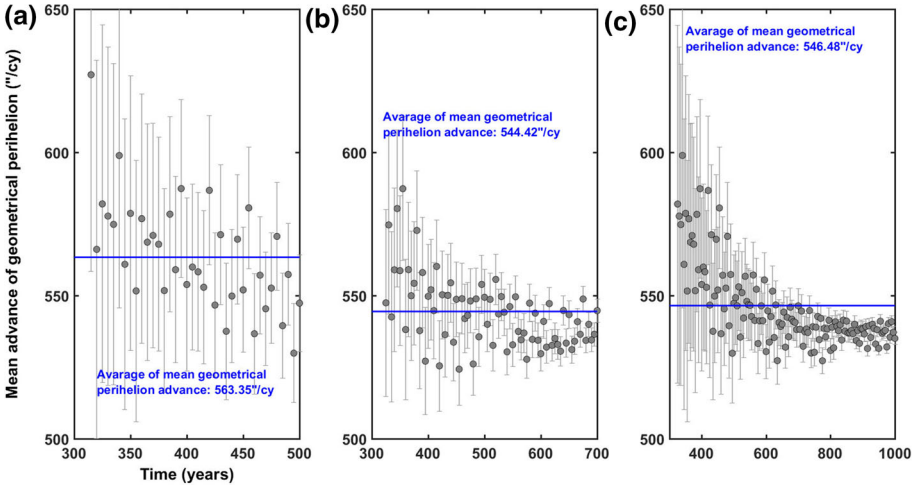

Fig. 11 Advance of the geometrical perihelion is fitted by the least squares method to a linear function. In Fig. 11a, b and c, the mean perihelion advance over a century is deduced by the fitting coefficients as a function of the fitting time interval for three different calculation intervals: 520 years, 718 years and 1011 years respectively. For each interval, the calculation of the mean advance of the perihelion per century is started on an initial fitting period of 300 years, that is gradually increased it with a step of 5 years

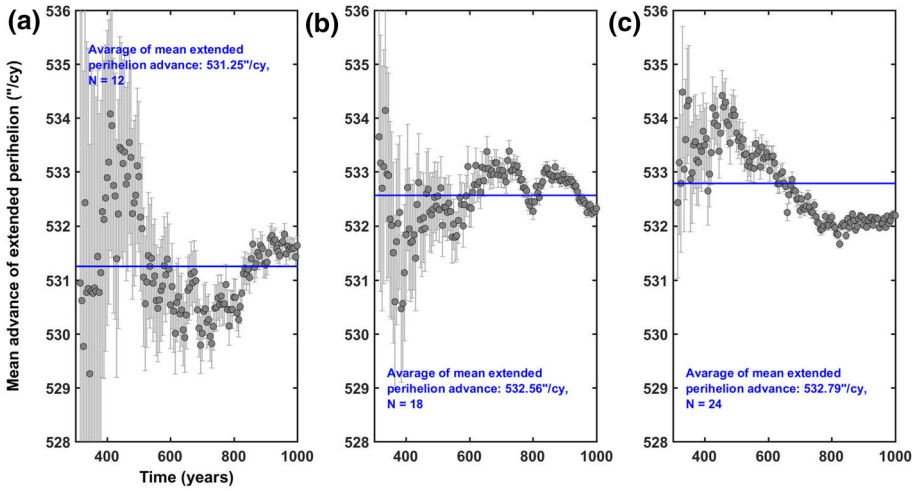

Fig. 12 Dependence of the mean extended perihelion advance per century on the number of points used during the integration is illustrated in Fig. 12. For the integration period of 1011 years, three curves corresponding to three different iteration steps (12, 18 and 24 iterations per day) are, respectively, plotted in Fig. 12a, b and c

In perspective, it is interesting to consider the long-term behavior of mean perihelion advance per century, on a scale of time interval for a few million years calculated by special algorithms for long-term orbital motion of the planets (Laskar et al. 2011). Future work will be needed to address this issue.

4 Conclusion

The study of the mean perihelion advance of Mercury by means of numerical methods within the framework of a model including only the non-relativistic Newtonian gravitational interactions of the solar system: eight major planets and Pluto in translation around the Sun shows the importance of the exact definition of the latter because of the open and not elliptic trajectory of Mercury.

The notions of extended and geometrical perihelia have been introduced to distinguish more precisely the differences with the concept of the perihelion for the two-body problem and N-body problem. Since the period of revolution of Mercury around the Sun is no longer a strictly periodic function with a fixed period, the concept of the mean period of revolution has been introduced from Fourier analyses.

By fitting a mean plane to the trajectory of Mercury in a time interval of one mean period, a mean elliptical trajectory has been introduced whose foci and perihelion positions define the concept of a geometrical perihelion. The extended perihelion is defined as the closest point to the Sun each time interval of one mean period. The behavior of the advance of these new perihelia is compared with the rotation of the LRL vector.

I have shown in this study that the mean perihelion advance of Mercury per century as deduced from the behavior of the LRL vector, as well as the mean advances of the extended and geometrical perihelion per century, will depend on the fitting time interval and for intervals on the order of 1000 years, will converge to a value of $532.1''$/cy. Giant planets such as Jupiter can strongly influence the advance of extended and geometrical perihelia, but have

little direct influence on the perihelion advance as calculated on the basis of the LRL vector rotation. It was also shown that the mean advance of the extended perihelion per century depends strongly on the time step used in the calculations, whereas the mean advance of the geometrical perihelion per century, as well as that deduced by the rotation of the LRL vector, will hardly depend on the time step used in our calculations.

Acknowledgements The author thanks Virginia Hekinian for her valuable help for improving the English of this manuscript.

References

Anderson, J.D., Slade, M.A., Jurgens, R.F., Lau, E.L., Newhall, X.X., Standish, E.M.: Radar and Spacecraft Ranging to Mercury between 1966 and 1988. Publ. Astron. Soc. Aust. **9**(2), 324–324 (1991). https://doi.org/10.1017/S1323358000024371

Anderson, J.D., Jurgens, R.F., Lau, E.L., Slade, M.A., III., Schubert, G.: Shape and orientation of mercury from radar ranging data. Icarus **124**(2), 690–697 (1996). https://doi.org/10.1006/icar.1996.0242

Arminjon, M.: Numerical solution of the inverse problem in classical celestial mechanics, with application to Mercury's motion. Meccanica **39**(1), 17–29 (2004). https://doi.org/10.1023/A:1026264517370

Biswas, A., Mani, K.: Simulation model for anomalous precession of the perihelion of Mercury's orbit. Open Phys. (2005). https://doi.org/10.2478/BF02476507

Bretagnon, P.: Theory for the motion of all the planets—the VSOP82 solution. Astron. Astrophys. **114**(2), 278–288 (1982)

Charvatova, I.: The solar motion and the variability of solar activity. Adv. Space Res. **8**(7), 147–150 (1988). https://doi.org/10.1016/0273-1177(88)90184-6

Cicalò, S., Schettino, G., Di Ruzza, S., Alessi, E.M., Tommei, G., Milani, A.: The BepiColombo MORE gravimetry and rotation experiments with the orbit14 software. Monthly Notices R. Astron. Soc. **457**(2), 1507–1521 (2016). https://doi.org/10.1093/mnras/stw052

Clemence, G.M.: The relativity effect in planetary motions. Rev. Modern Phys. **19**, 361–364 (1947)

Clemence, G.M.: On the system of astronomical constants. Astron. J. **53**, 169 (1948). https://doi.org/10.1086/106088

Davies, B.: Elementary theory of perihelion precession. Am. J. Phys. **51**(10), 909–911 (1983). https://doi.org/10.1119/1.13382

Ebner, D.: Comments on B. Davies's, "Derivation of perihelion precession". Am. J. Phys. **53**(4), 374–374 (1985). https://doi.org/10.1119/1.14171

Efroimsky, M., Goldreich, P.: Gauge freedom in the N—body problem of celestial mechanics. Astron. Astrophys. **415**(3), 1187–1199 (2004). https://doi.org/10.1051/0004-6361:20034058

Fienga, A.: Observations astrométriques des planètes et ajustement des théories analytiques de leur mouvement. Thèse de Doctorat, Observatoire de Paris, Paris (October 1999). https://www.imcce.fr/content/medias/publications/publications-recherche/theses-habilitations/docs/Fienga_These.pdf

Garavaglia, T.: The Runge-Lenz vector and Einstein perihelion precession. Am. J. Phys. **55**(2), 164–165 (1987). https://doi.org/10.1119/1.15237

Goldstein, H., Poole, C.P., Safko, J.L.: Classical Mechanics, 3. ed., [nachdr.] edn. Addison Wesley, San Francisco Munich (2008)

Gurfil, P.: Analysis of J 2-perturbed motion using mean non-osculating orbital elements. Celest. Mech. Dyn. Astron. **90**(3–4), 289–306 (2004). https://doi.org/10.1007/s10569-004-0890-x

Jose, P.D.: Sun's motion and sunspots. Astron. J. **70**, 193 (1965). https://doi.org/10.1086/109714

Landau, L.D., Lifšic, E.M.: The Classical Theory of Fields, 4. rev. engl. ed., repr edn. Course of theoretical physics / L. D. Landau and E. M. Lifshitz, vol. 2. Elsevier Butterworth Heinemann, Amsterdam Heidelberg (2010)

Laskar, J.: Secular evolution of the solar system over 10 million years. Astron. Astrophys. **198**(1–2), 341–362 (1988). https://doi.org/10.1093/mnras/stw052

Laskar, J., Gastineau, M.: Existence of collisional trajectories of Mercury, Mars and Venus with the Earth. Nature **459**(7248), 817–819 (2009). https://doi.org/10.1038/nature08096

Laskar, J., Fienga, A., Gastineau, M., Manche, H.: La2010 a new orbital solution for the long-term motion of the Earth. A&A **532**, 89 (2011). https://doi.org/10.1051/0004-6361/201116836

Le Guyader, C.: Solution of the N-Body Problem Expanded Into Taylor Series of High Orders. Applications to the Solar System Over Large Time Range. Astronomy and Astrophysics 272, 687–694 (1993). Provided by the SAO/NASA Astrophysics Data System

Le Verrier, U.J.: Theorie du mouvement de Mercure. Annales de l'Observatoire de Paris 5, 1–195 (1859). Paris : Mallet-Bachelier

Lo, K.-H., Young, K., Lee, B.Y.P.: Advance of perihelion. Am. J. Phys. **81**(9), 695–702 (2013). https://doi.org/10.1119/1.4813067

Loskutov, Y.M.: Comparison of theoretical and experimental data on the advance of the mercury perihelion: the proper contribution of the gravitational field of the sun to the perihelion advance. Moscow Univ. Phys. Bull. **66**(2), 129–134 (2011). https://doi.org/10.3103/S002713491102010X

Mazarico, E., Genova, A., Goossens, S., Lemoine, F.G., Neumann, G.A., Zuber, M.T., Smith, D.E., Solomon, S.C.: The gravity field, orientation, and ephemeris of Mercury from MESSENGER observations after three years in orbit. J. Geophys. Res. Planets **119**(12), 2417–2436 (2014). https://doi.org/10.1002/2014JE004675

Misner, C.W., Thorne, K.S., Wheeler, J.A., Kaiser, D.: Gravitation. Princeton University Press, Princeton, N.J (2017). OCLC: on1006427790

Narlikar, J.V., Rana, N.C.: Newtonian N-body calculations of the advance of Mercury's perihelion. Monthly Notices R. Astron. Soc. **213**(3), 657–663 (1985). https://doi.org/10.1093/mnras/213.3.657

Nobili, A.M., Will, C.M.: The real value of Mercury's perihelion advance. Nature **320**(6057), 39–41 (1986). https://doi.org/10.1038/320039a0

Park, R.S., Folkner, W.M., Konopliv, A.S., Williams, J.G., Smith, D.E., Zuber, M.T.: Precession of Mercury's Perihelion from Ranging to the MESSENGER Spacecraft. Astron. J. **153**(3), 121 (2017). https://doi.org/10.3847/1538-3881/aa5be2

Rana, N.C.: An investigation of the motions of the node and perihelion of Mercury. Astron. Astrophys. **181**, 195–202 (1987)

Roy, R.: A comparative study of the advance of the newtonian component of Mercury's perihelion by numerical analysis and perturbation theory. OALib **01**(06), 1–4 (2014). https://doi.org/10.4236/oalib.1100958

Rydin, R.A.: The theory of Mercury's anomalous precession. Proc. NPA **8**, 501–506 (2011)

Seidelmann, P.K., Observatory, U.S.N., Britain, G. (eds.) Explanatory Supplement to the Astronomical Almanac, Rev University Science Books, Mill Valley, Calif (1992)

Souami, D., Souchay, J.: The solar system's invariable plane. Astron. Astrophys. **543**, 133 (2012). https://doi.org/10.1051/0004-6361/201219011

Standish, E.M.: The observational basis for JPL's DE200, the planetary ephemerides of the astronomical almanac. Astron. Astrophys. **233**, 252–271 (1990)

Stewart, M.G.: Precession of the perihelion of Mercury's orbit. Am. J. Phys. **73**(8), 730–734 (2005). https://doi.org/10.1119/1.1949625

Taff, L.G.: Celestial Mechanics: A Computational Guide for the Practitioner. Wiley, New York (1985)

Vallado, D.A., McClain, W.D.: Fundamentals of Astrodynamics and Applications, 4th ed. edn. Space technology library. Microcosm Press, Hawthorne, Calif. (2013)

Verma, A.K., Fienga, A., Laskar, J., Manche, H., Gastineau, M.: Use of MESSENGER radioscience data to improve planetary ephemeris and to test general relativity. Astron. Astrophys. **561**, 115 (2014). https://doi.org/10.1051/0004-6361/201322124

Weinberg, S.: Gravitation and Cosmology: Principles and Applications of the General Theory of Relativity. Wiley, New York (1972)

Publisher's Note Springer Nature remains neutral with regard to jurisdictional claims in published maps and institutional affiliations.